Developmental Biology 348 (2010) 22–33

Contents lists available at ScienceDirect

Developmental Biology

journal homepage: www.elsevier.com/developmentalbiology

Zebrafish Nkd1 promotes Dvl degradation and is required for left–right patterning ☆

Igor Schneider [1,2], Patricia N. Schneider [1,3], Sarah W. Derry [1], Shengda Lin, Lacy J. Barton, Trudi Westfall, Diane C. Slusarski *

Department of Biology, University of Iowa, Iowa City, IA 52242, USA

ARTICLE INFO

Article history:
Received for publication 10 May 2010
Revised 22 August 2010
Accepted 27 August 2010
Available online 19 September 2010

Keywords:
Naked Cuticle
Dorsal forerunner cells
Kupffer's vesicle
Left–Right patterning
Cilia
Zebrafish

ABSTRACT

The establishment of the left–right (LR) axis in zebrafish embryos relies on signals from the dorsal forerunner cells (DFC) and the Kupffer's vesicle (KV). While the Wnt signaling network influences many aspects of embryonic development, its precise role in LR patterning is still unclear. One branch of the Wnt network leads to stabilization of β-catenin and activation of downstream target genes. Other Wnt ligands appear to act independently of β-catenin to modulate calcium release and influence cell polarity. Central to regulation of β-catenin and coordination of convergent extension (CE) movements is Dishevelled (Dvl). Naked Cuticle (Nkd) binds Dvl and modulates β-catenin-dependent and independent Wnt signaling. Here, we analyze the expression patterns of three zebrafish Nkd homologs and find enriched expression of *nkd1* in DFCs and KV. Dvl is degraded upon Nkd1 overexpression in zebrafish. Knockdown of Nkd1 specifically in the DFC results in β-catenin nuclear localization and transcriptional activation as well as alterations to DFC migration, KV formation, ciliogenesis and LR patterning. Furthermore, we identify asymmetric expression of the Nodal antagonist *charon* around the KV and show that Nkd1 knockdown impacts asymmetric *charon* expression. Our findings show that Nkd1 acts as a β-catenin antagonist in the DFCs necessary for LR patterning.

Introduction

As vertebrate embryos progress through early development and enter gastrulation, morphological differences with regard to the anterior–posterior (AP) and dorsal–ventral (DV) axes are already evident, yet the embryo appears bilaterally symmetric. In zebrafish, LR symmetry breaking involves a group of non-involuting dorsal mesoderm cells, the DFCs. The DFCs migrate ahead of the blastoderm margin during gastrulation (Cooper and D'Amico, 1996; Melby et al., 1996) and coalesce into a single rosette that differentiates into the KV (Oteiza et al., 2008). As they migrate, these cells express signaling molecules such as the Brachyury homolog *no tail*, *spade tail*, *polaris*, *pkd2* and *left–right dynein related 1* (*lrdr1*). DFC-specific knockdown of these gene products or ablation of the DFCs disrupts LR patterning (Amack and Yost, 2004; Essner et al., 2005).

Cilia in the lumen of the zebrafish KV and in the mouse node generate a leftward fluid flow (Essner et al., 2005; Kramer-Zucker et al., 2005; Nonaka et al., 1998). The cilia-driven flow, referred to as nodal flow, has also been described in rabbit, medakafish (Okada et al., 2005) and *Xenopus* embryos (Schweickert et al., 2007). KV/node cilia flow is thought to initiate molecular LR signals including the left-sided expression of the secreted TGFβ-related factor *nodal* (Reviewed in (Ahmad et al., 2004)) and downstream targets of *nodal* including *lefty1* and *pitx2* (Reviewed in (Hamada et al., 2002; Wright and Halpern, 2002). Left-sided gene expression in the lateral plate mesoderm (LPM), in turn, relays asymmetric information to internal organs as organogenesis commences. Asymmetric expression of *nodal* and its downstream targets are regulated by Charon, a member of the Cer/Dan class of Nodal antagonists. Zebrafish *charon* is expressed in cells around the KV (Hashimoto et al., 2004) and the murine Dante/Cerl-2 is expressed around the mouse node (Marques et al., 2004). It has been proposed that Cerl-2 regulation around the node, coupled to a reaction–diffusion system involving Nodal and Lefty, stabilizes the initial asymmetry in the LPM (Oki et al., 2009). Yet, the precise signaling mechanism linking nodal flow and KV/node asymmetric gene expression remains uncertain.

A notable aspect of the KV/node is the arrangement of its epithelial cells with cilia protruding from the apical surface. This display of morphological polarization has been characterized as a form of planar cell polarity (PCP) (Antic et al., 2010). Noncanonical Wnts, also referred to as β-catenin-independent Wnts, are involved in determining the alignment of hairs on the wings in *Drosophila*, and in

Abbreviations: Ca^{2+}, Calcium; Nkd, Naked Cuticle; DFC, Dorsal forerunner cells; KV, Kupffer's vesicle; LR, left–right; MO, Morpholino.

☆ The nkd3 sequence has been submitted to Genbank: accession HQ176463.

* Corresponding author. Department of Biology/246 Biology Building, Iowa City, IA 52242, USA. Fax: +1 319 335 1069.
E-mail address: diane-slusarski@uiowa.edu (D.C. Slusarski).
[1] These authors contributed equally.
[2] Present address: Department of Organismal Biology and Anatomy, University of Chicago, Chicago, IL, 60637, USA.
[3] Present address: Department of Neurobiology, The University of Chicago Medical Center, Chicago, IL, 60637, USA.

0012-1606/$ – see front matter © 2010 Elsevier Inc. All rights reserved.
doi:10.1016/j.ydbio.2010.08.040

vertebrates, modulating calcium release and coordinating CE movements during gastrulation (Wnt/PCP) (Kohn and Moon, 2005; Roszko et al., 2009; Solnica-Krezel, 2005). Recent reports indicate that proteins involved in β-catenin-independent Wnt signaling, including Vangl1 and Prickle2, play a role in establishing a polarized epithelium in the mouse, *Xenopus* and chick nodes (Antic et al., 2010; Zhang and Levin, 2009). In addition, Frizzled-2-mediated noncanonical Wnt signaling has been proposed to regulate ciliogenesis in the KV (Oishi et al., 2006) and Seahorse, a protein associated with cilia-mediated processes, binds Dvl and can promote Wnt/PCP signaling (Kishimoto et al., 2008). Yet, Wnt activity in early embryogenesis is cilia independent (Huang and Schier, 2009; Ocbina et al., 2009). Thus, the precise role of noncanonical Wnts in KV formation and LR asymmetry is yet to be determined.

Wnts of the so-called canonical pathway (Wnt/β-catenin) function by disabling a β-catenin-degradation complex, which includes APC, Axin and GSK3β, leading to β-catenin stabilization. Subsequently, stabilized β-catenin protein translocates to the nucleus and interacts with the members of the LEF/TCF transcription factor family to promote the activation of downstream target genes (Huang and He, 2008). The Wnt/β-catenin pathway has also been implicated in KV formation and LR patterning, as zebrafish Wnt3 and Wnt8 morphants have reduced KV size, shorter cilia, decreased *charon* expression and LR patterning defects (Lin and Xu, 2009). In addition, in the mouse node, Wnt3a signaling via β-catenin is required for expression of Pkd1 in mechanosensory cilia and for proper LR asymmetry (Nakaya et al., 2005). Interestingly, while the Wnt/β-catenin pathway has a role in KV function, it appears to be repressed earlier, during DFC migration. In fact, β-catenin activity is suppressed in the DFCs and misexpression of a constitutively active form of β-catenin in DFCs results in LR patterning defects (Schneider et al., 2008). Furthermore, DFC-specific knockdown of Axin, a Wnt/β-catenin antagonist, also leads to LR patterning defects (Schneider et al., 2008). Therefore, proper DFC migration, KV formation and LR patterning appear to involve both β-catenin-dependent and -independent Wnt signaling and thus may require potential mediators that can integrate signals from different arms of the Wnt network.

Among candidate mediators, Nkd displays the distinctive property of affecting both β-catenin-dependent and -independent arms of the Wnt signaling network. The *Drosophila nkd* has been shown to function as a Wg inducible antagonist (Zeng et al., 2000). The mechanism underlying Nkd-mediated antagonism of Wg involves binding to the basic/PDZ domain of Dvl, a scaffold protein that is central to both β-catenin-dependent and -independent Wnt pathways (Rousset et al., 2001). Mammals possess two Nkd homologs, Nkd1 and Nkd2 (Katoh, 2001; Wharton et al., 2001), which also interact with the basic/PDZ domain of Dvl and inhibit the Wnt/β-catenin pathway (Wharton et al., 2001; Yan et al., 2001). Various reports using cell culture assays indicate that Nkd-mediated Wnt antagonism involves Dvl degradation (Creyghton et al., 2005; Guo et al., 2009; Hu et al., 2010). Interestingly, overproduction of either mammalian or fly Nkd homologs leads to CE defects in *Xenopus* (Rousset et al., 2001; Yan et al., 2001) and zebrafish Nkd1 and Nkd2a were shown to antagonize both canonical and noncanonical Wnt signaling (Van Raay et al., 2007). Whether Nkd proteins function as a switch between different arms of Wnt pathways (Yan et al., 2001) or simply as antagonist of both pathways (Van Raay et al., 2007), Nkd activity may enable cells to translate converging canonical and noncanonical Wnt signaling cues into a distinct output.

Here we describe a novel zebrafish Nkd homolog Nkd3, and analyze Nkd expression during gastrulation. We find enriched zebrafish *nkd1* expression in DFCs and KV. We find that Dvl is degraded in zebrafish embryos upon *nkd1* overexpression. Conversely, DFC-specific knockdown of Nkd1 leads to upregulation of β-catenin and altered DFC migration. In addition, we show that Nkd1 knockdown leads to loss of cilia in the KV, followed by altered expression of asymmetric molecular markers and LR patterning defects. Furthermore, we identify asymmetric expression of the nodal antagonist *charon* around the KV and show that disruption of ciliary proteins affects *charon* asymmetry. Finally, we show that Nkd1 knockdown also disrupts *charon* asymmetry, likely by an impact on KV cilia. In conclusion, this study shows that zebrafish Nkd1 destabilizes Dvl and supports a role for Nkd1 antagonism of Wnt signaling in the DFCs, which are required for KV formation, normal ciliogenesis, asymmetric *charon* expression and LR patterning.

Materials and methods

Embryo manipulation

Zebrafish embryos were collected from natural spawning. Staging was according to Kimmel et al. (Kimmel et al., 1995). Live embryos were photographed after orienting in 3% methylcellulose.

Cloning of zebrafish Nkd

nkd clones were amplified from embryonic stage cDNA using the following primers: Nkd1 (full length): fwd, 5′- TTCTCAAGTGCTCTCCGATG; rev, 5′- TCTCCTGCTTGACTTTTCAGG. Nkd2a (partial): fwd, 5′-AGACAGGAGTGGGTTTTCACA; rev, 5′- TAGACGGCATCATGTCTGGT. Nkd3 (full length): fwd, 5′- TGAAGAATCGACATGGGAAAG; rev, 5′-AGAGTGTGTGGTTGGGTCAG. Protein sequence alignment was performed using ClustalX program (version 2.0.12) and percent identity was determined using SIM alignment Tool (http://ca.expasy.org/tools/sim-prot.html). For the Phylogenetic analysis, Nkd sequences were retrieved from public databases NCBI (www.ncbi.nlm.nih.gov) and Ensembl (www.ensembl.org). The following sequences and their respective accession numbers were included in the analysis: *Drosophila melanogaster* (DmNkd, FBpp0074806), *Danio rerio* (DrNkd1, AY863053; DrNkd2a, EF192161), *Homo sapiens* (HsNkd1, NM_033119; HsNkd2, NM_033120) , *Mus musculus* (MmNkd1, NM_027280; MmNkd2, NM_028186), *Gallus gallus* (GgNkd1, ENSGALP00000005967), *Takifugu rubripes* (TrNkd1, ENSTRUP00000020681; TrNkd2, ENSTRUP00000036718), *Xenopus tropicalis* (XtNkd1, ENSXETP00000039973), *Gasterosteus aculeatus* (GaNkd1, ENSGACP00000022069; GaNkd2, ENSGACP00000011299), *Oryzias latipes* (OlNkd1, ENSORLP00000017425; OlNkd2, (ENSORLP00000010101), *Anopheles gambiae* (AgNkd, BK005845), and *Saccoglossus kowalevskii* (SkNkd, GU076049). A neighbor joining phylogenetic tree was constructed and visualized using NJPlot and Dendroscope programs.

Antisense oligonucleotide-mediated knockdown

MOs were purchased from Gene Tools, LLC. Control: CCTCTTACCTCAGTTACAATTTATA, Nkd1splice acceptor: CTATCGCCTAAAACAAGAAAACACG; Nkd1splice donor: AGAGTCCTGAAGGTGAGTTGAGTGT; Nkd1met: GATGCAGAGAAATGGGTAAACTTCA; Nkd2a splice acceptor: CACTCCAGATCCTGACAGATCACAC; Nkd3UTR: GCTTGTGTCAGAAGTTGTGCATCTC; Nkd3met: CATGTTTGGATTGCAGCTTTCCCAT; Ift88: CAACTCCACTCACCCCATAAGCTGT; Invs: CAACGCCGTCTGCTGTAGAACAAAC; seahorse: TCAGATCCTCACTGATGCGGACCAT. MO (8 ng) or *in vitro* transcribed RNA (*nkd1*, zebrafish *dlv2-myc*, *Xenopus dvl*-GFP) at 70–100 ng/μl were injected into the yolk of 1-cell-stage or DFC-targeted in the 512-cell-stage embryo. For assessment of MO-mediated knockdown efficiency, cDNA generated from 4 hpf MO-injected embryos were amplified by RT-PCR using *nkd1* primers: fwd, 5′-GATGCAGAGAAATGGGTAAACTTCA; rev, 5′-TCTTCTTCCACTGATACAGCACA and β-actin primers: fwd, 5′-TCAGCCATGGATGATGAAAT-3′; rev, 5′-GGTCAGGATCTTCATGAGGT-3′ as control.

Whole-mount in situ hybridization (WMISH) and LR scoring

For all manipulations, embryos were fixed in 4% paraformaldehyde/1× PBS. Digoxygenin-labeled antisense RNA riboprobes (Roche) were synthesized using linearized templates and the appropriate RNA polymerase. Hybridization as described (Schneider et al., 2008).

DFC migration in the Dusp6:d2EGFP transgenic line was assessed by WMISH with EGFP riboprobe. β-catenin transcriptional activation was evaluated by TopdGFP (Dorsky et al., 2002) expression in the DFC and by *axin2* (Shimizu et al., 2000; Weidinger et al., 2005). Zebrafish cardiac jogging was assessed in live embryos at 28 hpf by DIC optics and by WMISH with *nkx2.5*. CE was assessed by WMISH with *krox20* and *myoD*. KV was analyzed in live embryos at 8–10 somite stage by light microscopy and by WMISH with *charon*. Molecular asymmetry was assessed at 18–22 somite stage by WMISH with spaw or combined *lefty1* and *lefty2* (as described in (Schneider et al., 2008)). Scorers were masked to the treatment of the embryos.

Statistical analysis

For statistical analysis of *charon* asymmetry, left and no bias were considered altered, right bias *charon* enrichment was considered normal. Fisher's Exact Test computation was performed compared to wild type (wt). For β-catenin nuclear localization, MO-injected was compared back to uninjected using Fisher's exact test. For Axin 2 and TOPdGFP analysis, expression patterns of wt embryos were defined as normal. Embryos demonstrating ectopic or expanded expression were classified as altered. Fisher's Exact Test computation was performed compared to control MO-injected embryos. p-values smaller than 0.01 were considered statistically significant.

Immunolocalization

Immunofluorescence was performed according to a standard protocol. Multichannel confocal microscopy was used to evaluate Topro 3 and Dvl-GFP localization. Dusp6:d2EGFP transgenic embryos were used to locate the KV with anti-acetylated tubulin staining. Analysis of β-catenin (Sigma) distribution was followed by fluorescent secondary antibody (Alexa Fluor 488, Molecular Probes) or conjugated anti-horseradish peroxidase (Jackson ImmunoResearch). The DFC regions were identified on the confocal by mounting gsc-GFP transgenic embryos (Doitsidou et al., 2002) in low melt agarose. Embryos were imaged on the Leica SP2 AOBS scanning laser confocal microscope system with 63× magnification.

Western blot

Embryos at the 1–2 cell stages were injected with C-terminal myc-tagged zebrafish *dvl2* (50 pg) alone, with *EGFP* (150 pg), and with *nkd1* (150 pg) RNA. Nkd1 and Dvl2 were cloned into Tol2kit p3E-MTpA, by Multisite Gateway cloning (Invitrogen, CA). At 80% epiboly (8.5 hpf), embryos were lysed in phosphoprotein buffer (80 mM ß-glycerophosphate pH 7.0, 20 mM EGTA, 15 mM MgCl2, 1 mM DTT, 1 mM PMSF, 1:50 protease inhibitor cocktail; Sigma) and cleared by centrifugation at 15,000 *g*. 10 µl loading buffer per embryo was added to the cell lysate. One embryo equivalent was run on a pre-cast 10% Tris HCL protein gel (Bio-Rad Laboratories) for 105 min at 100 V. The protein was transferred to a nitrocellulose membrane for 1 h at 400 mA. The membrane was blocked in milk blocking buffer for 1 h and then probed with mouse anti-Myc antibody (9E10, Santa Cruz Biotechnology, Santa Cruz, CA) diluted 1:1500 in blocking buffer (1× PBS, 0.15 molar NaCl, 0.1% Tween 20, 0.04 g/ml of dried milk) overnight at 4 °C. Anti-β-actin antibody (Sigma-Aldrich) diluted 1:2000 was used for loading control.

Results

Nkd expression in the DFC and KV

We have previously identified calcium (Ca^{2+}) release activity in the DFC region and shown that DFC targeting of Ca^{2+} release inhibitors alters DFC migration and results in upregulation of β-catenin-dependent transcription (Schneider et al., 2008). Therefore, genes that modulate β-catenin activity would serve as candidate mediators of signaling in the DFC. Given the central role of Nkd in modulating Wnt signaling outputs, we characterized the expression of zebrafish Nkd homologs relative to DFC and KV. For this study, we analyzed the expression of two previously identified zebrafish Nkd homologs, Nkd1 and Nkd2a (Van Raay et al., 2007), in addition we identified a novel *nkd* homolog, Nkd3. Sequence alignment indicates that Nkd3 amino acid sequence shows greater similarity to Nkd2a (40% identity) than to Nkd1 (30% identity), whereas Nkd1 and Nkd2a are 37% identical (supplemental Fig. 1A). Phylogenetic analysis groups Nkd3 with vertebrate Nkd2 homologs (supplemental Fig. 1B). The three *nkd* transcripts have overall global expression (Figs. 1A–O). There is maternal expression of *nkd2a* (Fig. 1F) and *nkd3* (Fig. 1K) but not *nkd1* (Fig. 1A). At the somite stages, localized expression for *nkd1*, *nkd2a* and *nkd3* is observed in KV progenitor cells (Figs. 1C, D, H, I, M, N). In contrast to *nkd2a* and *nkd3*, DFC-specific expression of *nkd1* becomes more pronounced as these cells migrate to the tailbud (Figs. 1P–S).

Nkd1 function is required for KV formation and organ laterality

Since we find enriched levels of *nkd1* in the DFC and localized expression of all three nkds in the KV region, we set out to evaluate the contributions of Nkd to LR patterning. We evaluated the knockdown efficiency of a splice-block antisense morpholino oligonucleotide injected in the 1-cell stage and RNA isolated at the blastula stage by RT-PCR. Shown for Nkd1MO injected embryos, we observe partial knockdown with additional bands (Fig. 2A) that demonstrate both inclusion of intron 2, and exclusion of exon 3. Sequence analysis confirmed that each caused premature stops in the open reading frame (data not shown). Since Nkd1 has functions in other tissues, global knockdown led to severe defects at epiboly stages, preventing appropriate evaluation of laterality (data not shown), we utilized an injection technique to target the MO to the DFCs (Amack and Yost, 2004) to avoid the severe effects caused by global Nkd knockdown. MO or control reagents delivered to the yolk by late stage injection are taken up by the DFC and found in the KV (Figs. 2B and C). DFC-targeted embryos were evaluated for KV formation. Morphological analysis in live wild type (wt) and control MO-injected embryos at 8–12 somite stages reveals the crater-like KV structure in the tailbud of the embryos that is wider than the notochord (Figs. 2D and E). DFC-knockdown of Nkd1 resulted in altered KV formation (Fig. 2F), with 47% embryos showing reduced or absent KV (Fig. 2G), whereas DFC-knockdown of Nkd2 and Nkd3 did not substantially disrupt KV formation (Fig. 2G). The impact of Nkd1 knockdown in the DFC was confirmed with two additional MOs (splice donor MO and met MO) and is consistent with the enriched *nkd1* expression in the DFC.

To rule out a later role for Nkd2 and Nkd3 in LR, we evaluated organ laterality in knockdown embryos. In uninjected and control-injected embryos, the heart migrates to reside on the left side (Fig. 2H), whereas DFC-knockdown of Nkd1 caused aberrant cardiac phenotypes, including no jog, right jog, and *cardia bifida* (Figs. 2I–L). DFC-targeted knockdown with Nkd2MO or Nkd3MO did not disrupt jogging (Fig. 2L). Since Nkd2MO or Nkd3MO did not significantly disrupt KV (Fig. 2G) or heart jogging (Fig. 2L), we focused our studies on Nkd1.

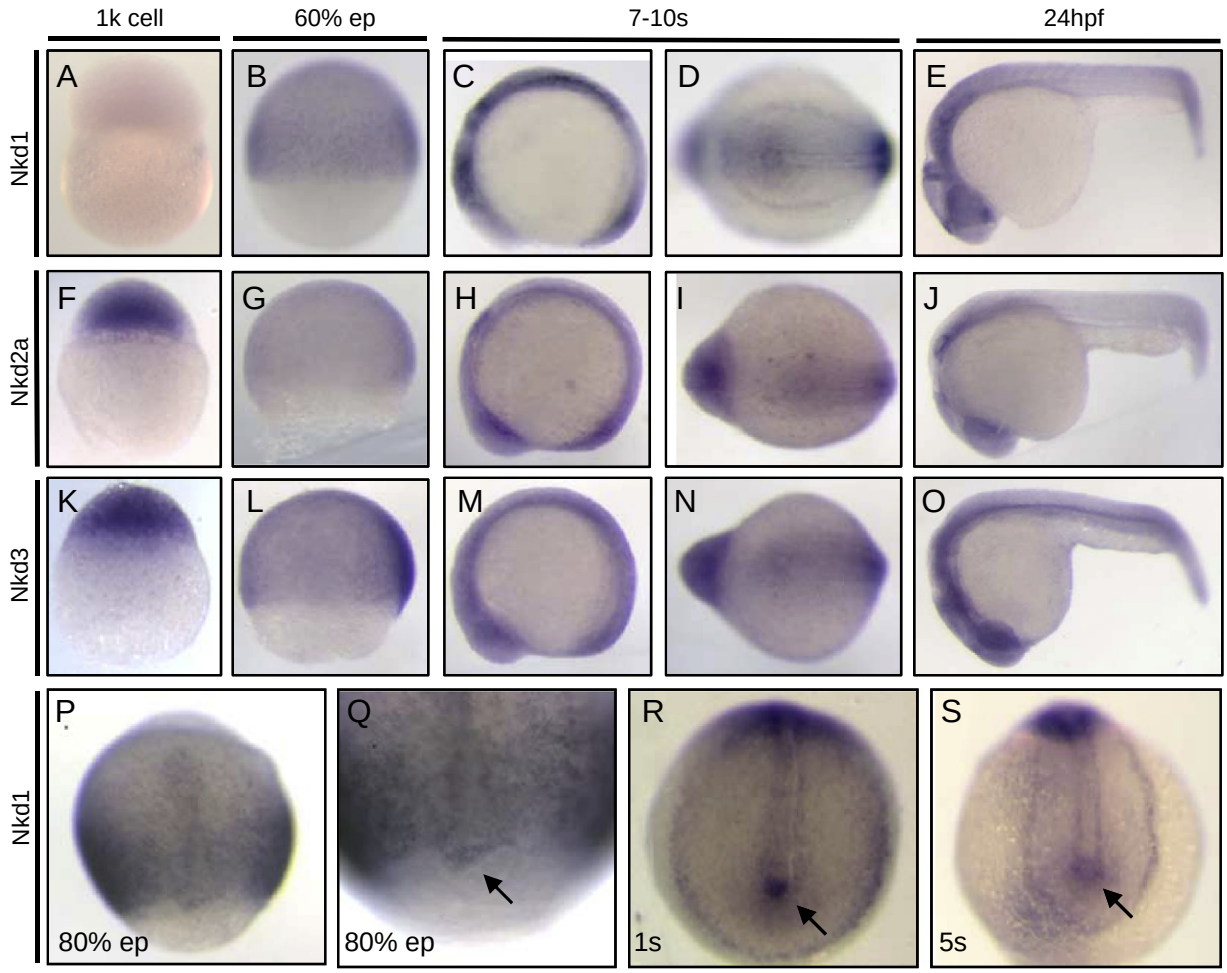

Fig. 1. Expression pattern of zebrafish Nkd homologs. *nkd1* expression is not detectable at 1k-cell stage (A) but ubiquitous during epiboly (B). During somite stages, *nkd1* is expressed in somites, rhombomeres and tailbud at 4-somite stage (C) and in cells around the forming KV (D). *nkd1* expression at 24 hpf (E). *nkd2a* is ubiquitously expressed during 1k-cell stage (F), epiboly (G), and in somites, rhombomeres and tailbud at 4-somite stage (H). *nkd2a* expression in tailbud (I) and at 24 hpf (J). nkd3 ubiquitously expressed during 1k-cell stage (K), epiboly (L), and in somites (M). *nkd3* expression in tailbud (N) and at 24 hpf (O). (P–S) *nkd1* is expressed ubiquitously throughout gastrulation (P) and in the DFCs at 80% epiboly (Q). At 1-somite stage, marked nkd1 expression is observed the tailbud (R), and in cells around the KV (S). Arrows denote DFCs during 80% epiboly, tailbud and 5-somite stage. hpf = hours post fertilization.

Nkd1 knockdown alters DFC migration and KV cilia formation

The DFCs migrate to the tailbud to form the ciliated KV. DFCs in Ca^{2+} inhibited embryos migrate to the tailbud, similar to controls, but then disperse from the normal migration path (Schneider et al., 2008). To determine whether Nkd1 knockdown disrupted DFC migration, we monitored the DFC distribution using the *Dusp6:d2EGFP* transgenic (Molina et al., 2007) which expresses EGFP in a fibroblast growth factor (FGF)-responsive manner in several tissues including the DFC and KV. At discrete time-points between 80% epiboly to eight-somite stage, control or Nkd1MO^{DFC} injected embryos were fixed for whole-mount *in situ* hybridization with an EGFP probe. During epiboly, the DFCs appear as a tight cluster of cells in wt and in Nkd1MO^{DFC} embryos (Figs. 3A and B). At somite stages, DFCs form a compact cluster at the midline (Fig. 3C) whereas Nkd1MO^{DFC} embryos displayed a smaller cluster at the midline with other cells randomly dispersed (Fig. 3D). At eight-somite stage in wt, the EGFP-expressing DFCs form a circular KV (Fig. 3E). Consistent with the morphological observation of reduced/absent KV, Nkd1MO^{DFC} embryos form a markedly smaller EGFP-expressing domain and dispersed DFC cells (Figs. 3F and I). To determine the cilia content of the KV, we performed anti-acetylated tubulin staining. Confocal analysis of *Dusp6:d2EGFP* transgenic embryos reveal that EGFP-expressing cells in the wt KV also have cilia (Fig. 3G). In Nkd1MO^{DFC} injected embryos *Dusp6:d2EGFP* transgenic embryos, not only is there reduced EGFP-expressing cells in the KV but also reduced cilia formation (Fig. 3H). In conclusion, Nkd1 knockdown in DFCs results in DFC dispersal, reduced KV size and cilia.

Asymmetric charon expression around the KV requires Nkd1 function

We next investigated the function of Nkd1 in the DFC/KV with molecular markers. *charon*, a Cer/Dan Nodal antagonist, is expressed in cells forming a horseshoe shape around the posterior zebrafish KV (Hashimoto et al., 2004). *charon* inhibits expression of the Nodal related gene spaw and its downstream targets *lefty1* and *lefty2* (*lefty1/2*) on the right side lateral plate mesoderm (LPM) but not on the left side (Hashimoto et al., 2004). Although the mechanism of the right-sided bias for nodal antagonism is not well defined, asymmetric *charon* expression across the KV has been described in Medaka (Hojo et al., 2007). We first investigated *charon* expression in 8- to 10-somite-stage uninjected zebrafish embryos and found a similar *charon* expression bias on the right side of the KV (Fig. 4A). We also evaluated *charon* expression in CtrlMO^{DFC}-injected zebrafish embryos and found stronger expression on the right side of the KV (Fig. 4B). Interestingly, upon Nkd1MO^{DFC} knockdown, *charon* expression is largely symmetric, with 62% of embryos showing no expression bias (Figs. 4C and G). DFC-targeted co-injection of *nkd1* RNA mixed with Nkd1MO can significantly restore asymmetric distribution of *charon* (Fig. 4G). Thus,

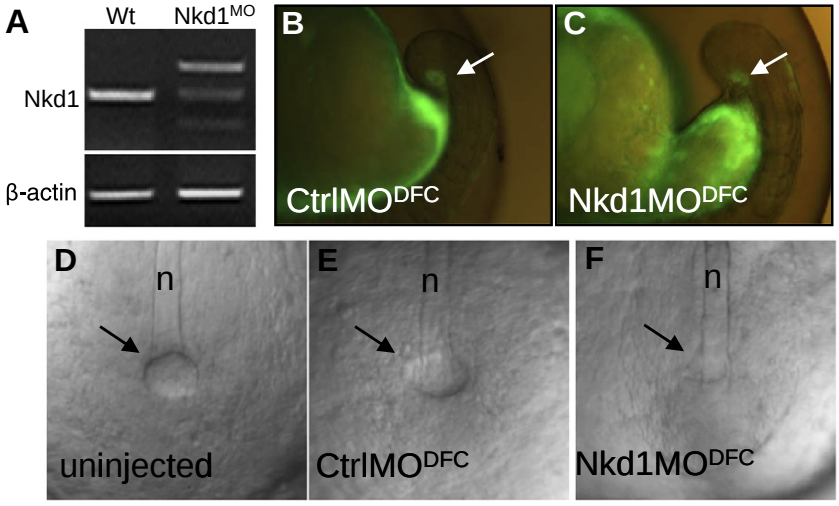

G		Kupffer's Vesicle morphology (%)		
Group	n	Normal	Reduced	Absent
Wt	126	98	2	0
CtrlMO^{DFC}	189	92	8	0
Nkd1MO^{DFC}	331	53	36	11
Nkd2MO^{DFC}	49	92	8	0
Nkd3MO^{DFC}	41	85	15	0

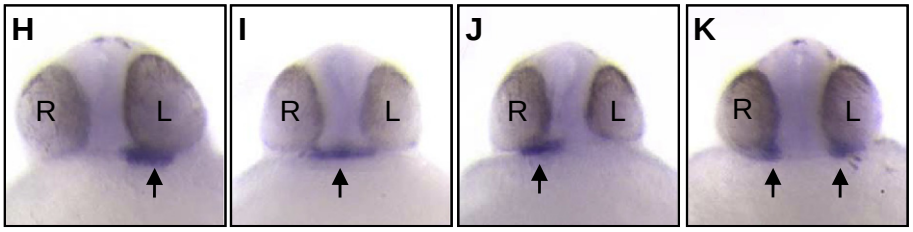

L		Cardiac Jogging (%)			
Group	n	Left Jog	Right Jog	No Jog	*Cardia Bifida*
Wt	78	100	0	0	0
CtrlMO^{DFC}	62	94	3	3	0
Nkd1MO^{DFC}	151	38	28	15	19
Nkd2MO^{DFC}	43	93	2	5	0
Nkd3MO^{DFC}	36	92	0	8	0

Fig. 2. Heart laterality defects after Nkd1 knockdown in DFCs. (A) RT-PCR using cDNA from wt or Nkd1MO-injected embryos: β-actin or Nkd1 were amplified. (B and C) Arrows denote efficient targeting of CtrlMO and Nkd1MO into the DFCs. (D–F) Bright field image of KV in wt (D), CtrlMO^{DFC} (E) and Nkd1MO^{DFC} (F) embryos, at 10-somite stage. Arrows indicate vesicle location; n = notochord. (G) Summary of KV morphology defects. (H–K) Arrows denote expression of *nkx2.5* in the heart, on the left side in wt (H) and on the middle (I), right (J) and bilaterally (K) in Nkd1MO^{DFC} embryos. (L) Summary of cardiac jogging defects.

Nkd1 function in the DFC is necessary for proper asymmetric *charon* expression.

The KV cilia have been postulated to create a directional fluid flow, ultimately generating an asymmetric signal (Essner et al., 2005; Kramer-Zucker et al., 2005) and in Medaka, asymmetric *charon* expression is cilia-dependent (Hojo et al., 2007). To test whether zebrafish asymmetric *charon* expression is cilia-dependent, we targeted three ciliary proteins known to be required for correct LR patterning: Inversin (Invs), Seahorse (Sea) and Polaris (Ift88) (Bisgrove et al., 2005; Kishimoto et al., 2008; Otto et al., 2003; Serluca et al., 2009; Sun et al., 2004). KV formation appears unaffected based on analysis of morphology (data not shown). However, MO-knockdown of each protein led to unbiased *charon* expression around the KV (Figs. 4D–G). Therefore, we conclude that asymmetric *charon* expression around the KV is cilia-dependent in zebrafish. Since we found that Nkd1MO^{DFC} resulted in reduced cilia number, we conclude that loss of *charon* asymmetry in Nkd1MO^{DFC} embryos is likely due to loss of KV cilia.

Asymmetric charon expression may be necessary for inhibition of Nodal on the right LPM and allow left-sided expression of *southpaw* (*spaw*). Therefore we evaluate the expression of *spaw* and downstream targets *lefty1/2* as a result of Nkd1 knockdown. In uninjected

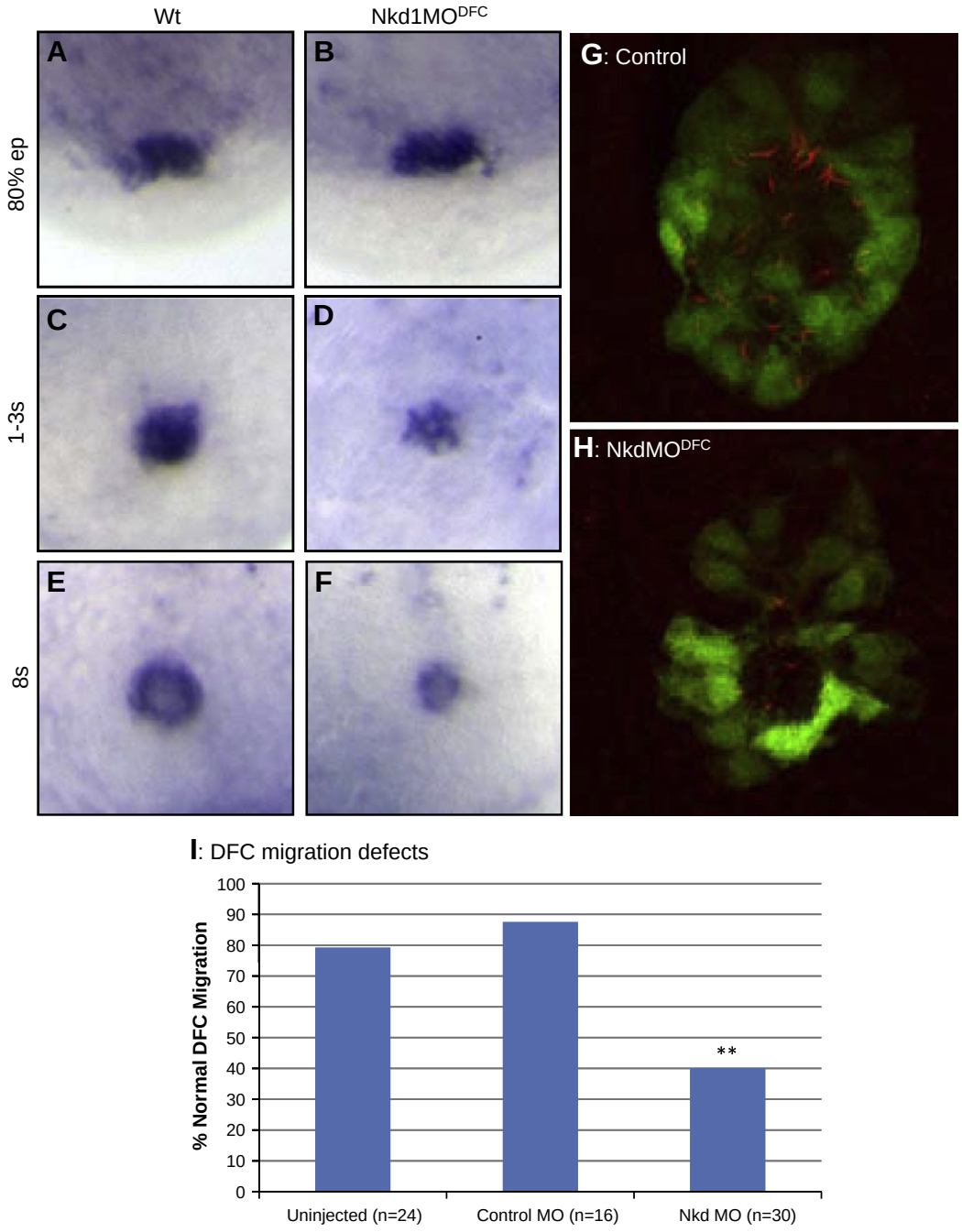

Fig. 3. Nkd1 is required for proper DFC migration and KV formation. (A–F) EGFP (Dusp6:d2EGFP) expression in wt (A, C and E) and Nkd1MO^{DFC} (B, D and F) embryos; DFCs were assessed at 80% epiboly (A and B), tailbud to 1-somite stage (C and D) and at 8-somite stage (E and F). (G and H) Fluorescence image denoting KV cilia in wt (J) and Nkd1MO^{DFC} (K) embryos. Dusp6:d2EGFP (green) and anti-acetylated tubulin (red) indicate cilia in KV cells. (I) Graph of DFC migration defects. N notes the sample size. ** = $p<0.01$ compared to uninjected using Fisher's exact test.

and Control^{DFC}-targeted embryos, we observe predominantly left-sided LPM expression of *spaw* (Figs. 5A, B and G) and *lefty1/2* (Figs. 5D, E and G). *spaw* and *lefty1/2* were mostly bilateral in Nkd1MO^{DFC} embryos (Figs. 5C, F and G). Bilateral expression of *spaw* and its downstream targets *lefty1/2*, as opposed of loss-of-expression, suggests that LR defects observed with Nkd1 knockdown are due to ectopic *spaw* expression that would otherwise be inhibited by *charon* on the right side. Therefore Nkd1 regulates LR patterning by consolidating asymmetric expression of *charon*. We next explore the mechanism of Nkd1 action in zebrafish.

Nkd1 overexpression promotes Dvl degradation and inhibits CE movements

Nkd binds to Dvl (Rousset et al., 2001) and vertebrate Nkds promote Dvl degradation in cell culture (Guo et al., 2009; Hu et al., 2010). To determine if zebrafish Nkd1 promotes Dvl turnover *in vivo*, we generated tagged *dvl2-myc* to express in zebrafish embryos alone or coinjected with either *nkd1* RNA or control RNA. Injected embryos were lysed at gastrula stages for western blot analysis and Dvl2-myc protein can be readily detected when injected alone or with control

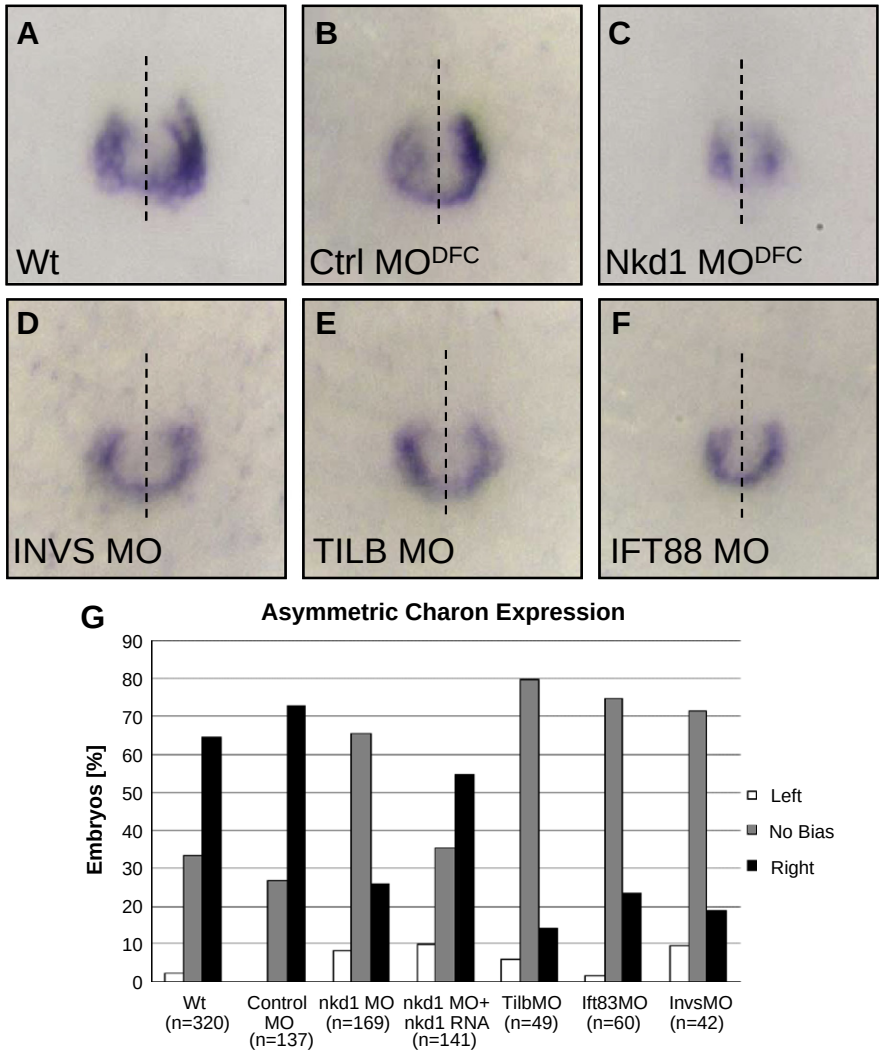

Fig. 4. Asymmetric *charon* expression around the KV is dependent on Nkd1 and cilia function. Expression of *charon* in wt (A), CtrlMO^{DFC} (B), and Nkd1MO^{DFC} (C) embryos. Expression of *charon* in InvsMO (D), SeaMO (E), and Ift88MO (F) injected embryos. Dashed line represents embryonic midline. (G) Graph of percent of embryos displaying left-sided (white bar), no bias (shaded bar) or right-sided biased (black bar) *charon* expression around KV. (n) notes the sample size for each injection set. ** = $p > 0.01$ compared to wt using Fisher's exact test. Nkd1MO^{DFC} p-value = 3.07×10^{-16}; Nkd1MO^{DFC} + *nkd1* RNA p-value = 0.01, SeaMO p-value = 2.3×10^{-11}; Ift88MO p-value = 3.5×10^{-9}; InvsMO p-value = 2.11×10^{-8}.

RNA (Fig. 6A). Co-injection of *dvl2-myc* with *nkd1* results in a marked decrease in the amount of Dvl2-myc protein (Fig. 6A). Consistent with western blot results, embryos injected with Dvl-GFP show broad expression when injected alone (Fig. 6B and C, left). In contrast, little or no Dvl-GFP expression could be detected in embryos coexpressing *dvl* and *nkd1* (Fig. 6B and C, right). To evaluate Nkd1-induced Dvl localization, we coexpressed *dvl-GFP* with *nkd1* and performed confocal analysis in whole embryos. Dvl-GFP alone appears as puncta in the cytoplasm (Fig. 6D), whereas coinjection of *dvl-GFP* with *nkd1* results in a noticeable decrease in GFP fluorescence and with faint plasma membrane localization (Fig. 6E).

Dvl plays a role in coordinating convergent and extension (CE) movements to thicken (dorsal convergence) and elongate (axis extension) the embryo (Keller, 2002). Consistent with Nkd misexpression inducing Dvl degredation, mouse Nkd1 induced CE defects in *Xenopus* overexpression assays (Yan et al., 2001) and overexpression of *nkd1* RNA in *wnt11/slb* zebrafish mutants exacerbated the slb phenotype (Van Raay et al., 2007). Therefore, we tested whether misexpression of zebrafish Nkd1 can disrupt CE movements. The anterior–posterior extension of the zebrafish hindbrain can be monitored by *krox20* expression in rhombomeres 3 and 5 (Fig. 6F), while in the trunk region the spacing and lateral expansion of somites is denoted by *myoD* expression (Fig. 6G). Overexpression of *nkd1* RNA induced CE defects, demonstrated by more closely spaced, yet expanded lateral domains of rhombomeres (Fig. 6H) and somites (Fig. 6I). Taken together, these observations indicate that zebrafish Nkd1 misexpression can impact CE movement and is sufficient to impact Dvl localization and stability. We next explore the mechanism of Nkd action in the zebrafish DFC.

Nkd1 knockdown leads to increased nuclear β-catenin and β-catenin target gene expression

Dvl is a key regulator of the β-catenin-degradation complex and since Nkd misexpression induced Dvl degredation, we assessed β-catenin levels in DFCs of Nkd1MO^{DFC}-injected embryos. Using the gsc-GFP transgenic line that decorates the midline during epiboly (Doitsidou et al., 2002) the DFC region is readily identified, shown here with anti-E-cadherin (Fig. 7A). While membrane associated β-catenin is found in all cells, cytoplasmic β-catenin is readily sequestered and targeted for degradation. In control 70–80% epiboly stage embryos, an average of 7% of the cells in the DFC cluster display β-catenin-positive nuclei (Figs. 7B and D). In contrast in Nkd1MO^{DFC}-injected embryos, we observed a statistically significant increase (20%, p-value $< 6.8 \times 10^{-6}$) of cells in the DFC cluster with β-catenin-positive nuclei (Figs. 7C and D). To confirm that nuclear β-catenin

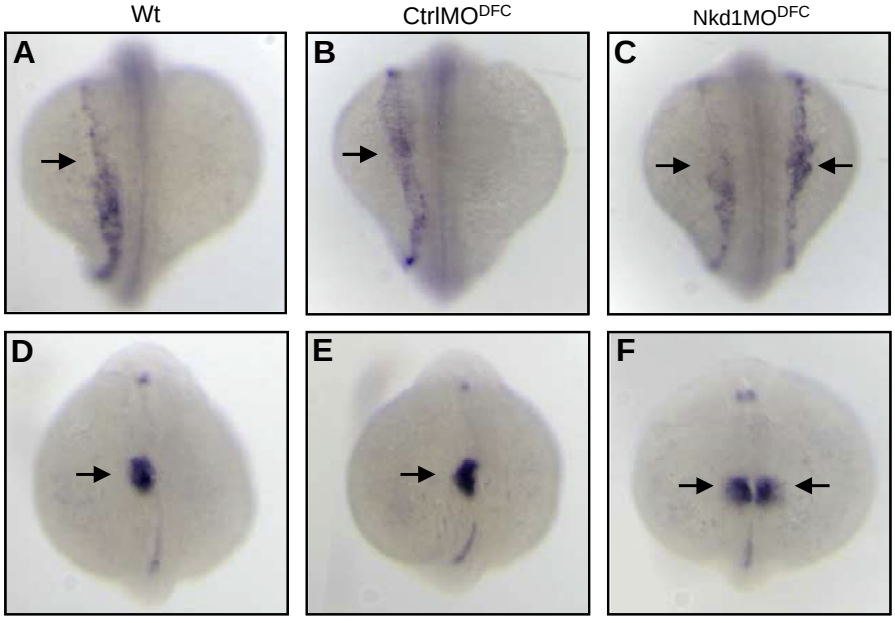

G

Marker	Group	n	Lateral plate (%) Left	Bil	Right	Absent
	Wt	39	100	0	0	0
spaw	CtrlMO^{DFC}	41	93	7	0	0
	Nkd1MO^{DFC}	138	33	61	6	0
	Wt	56	96	4	0	0
lefty1&2	CtrlMO^{DFC}	84	85	12	0	3
	Nkd1MO^{DFC}	112	35	46	10	9

Fig. 5. Nkd1 is required for asymmetric expression in the LPM. (A–C) Arrows denote left-sided *spaw* expression in wt (A), CtrlMO^{DFC} (B), and bilateral expression in Nkd1MO^{DFC} (C). Arrows denote left-sided *lefty1&2* expression in wt (D), CtrlMO^{DFC} (E), and bilateral expression in Nkd1MO^{DFC} (F). (G) Summary of spaw and *lefty1&2* asymmetric gene expression patterns.

correlated with increased transcriptional activity *in vivo*, we targeted Nkd1MO or ControlMO to the DFC region to analyze expression of the β-catenin target axin2 (Weidinger et al., 2005) and targeted Nkd1MO or ControlMO to the DFC region of transgenic embryos expressing destabilized GFP under the control of a β-catenin-responsive promoter, TOPdGFP (Dorsky et al., 2002). In ControlMO-injected embryos, there was active Wnt/β-catenin signaling in ventral–lateral domains, reflected by robust *axin2* expression (Fig. 7E) and TOPdGFP expression (supp. Fig. 2A) with minimal signal in the DFC region at 80% epiboly (Fig. 7E and supp. Fig. 2B). Nkd1MO-injected embryos show expanded axin2 expression (Fig. 7F) as well as ectopic GFP expression in the DFCs (Supp. Fig. 2C and D). Therefore Nkd function in the DFC influences β-catenin-dependent transcriptional activity and subsequent DFC migration and KV formation.

Discussion

In the DFCs, Ca^{2+} release antagonizes β-catenin and is required for DFC polarized migration, KV formation and LR patterning (Schneider et al., 2008). In addition, Axin knockdown in the DFC leads to laterality defects (Schneider et al., 2008). Therefore, we focused our studies on potential Wnt/β-catenin antagonists expressed in DFCs that could play a role in LR patterning. For this reason, we analyzed the expression of the two previously identified zebrafish Nkd homologs, Nkd1 and Nkd2a, and cloned an additional Nkd homolog, Nkd3. Amino acid sequence alignment, expression data and phylogenetic analysis suggest that Nkd3 is most closely related to Nkd2a, and likely a product of teleost-specific genome duplication (Amores et al., 1998; Jaillon et al., 2004; Taylor et al., 2003). Whereas all Nkd transcripts were mostly ubiquitously expressed during gastrulation, Nkd1 displayed enriched expression in the migrating DFC cluster and around KV. Consistent with the expression patterns, knockdown of Nkd1 in DFCs, but not Nkd2a or Nkd3, resulted in heart laterality defects.

Studies have noted that Ca^{2+} release is an output of both Wnt/Ca^{2+} and components of the Wnt/PCP pathway (reviewed by (Slusarski and Pelegri, 2007)). In addition, Ca^{2+} release can negatively regulate or limit Wnt/β-catenin signaling (Topol et al., 2003; Westfall et al., 2003a, b). Hence, β-catenin-independent Wnt signaling has been characterized as a complex network with cellular outputs defined by Ca^{2+} modulation, polarized cell movement and Wnt/β-catenin antagonism (Freisinger et al., 2008; Slusarski and Pelegri, 2007). The DFCs display all of the above-mentioned properties of noncanonical Wnt outputs, which include the Ca^{2+} release activity that controls β-catenin levels and DFC polarized migration. Nkds can impact both β-catenin-dependent and -independent Wnts and may in fact act at the interface between Wnt pathways. Here, we find that Nkd1 knockdown in DFCs, much like Ca^{2+} inhibition, results in nuclear β-catenin accumulation, aberrant DFC migration and defective KV formation, followed by LR patterning defects. We show that Nkd1, like its mammalian homologues, can impact CE movements and promote Dvl degradation (Guo et al., 2009; Hu et al., 2010; Van Raay et al., 2007; Wharton et al., 2001). Our results suggest that Nkd1 exerts its effects in part by regulating Dvl stability, identifying a possible mechanism for Nkd1-mediated impact in β-catenin in DFCs and KV.

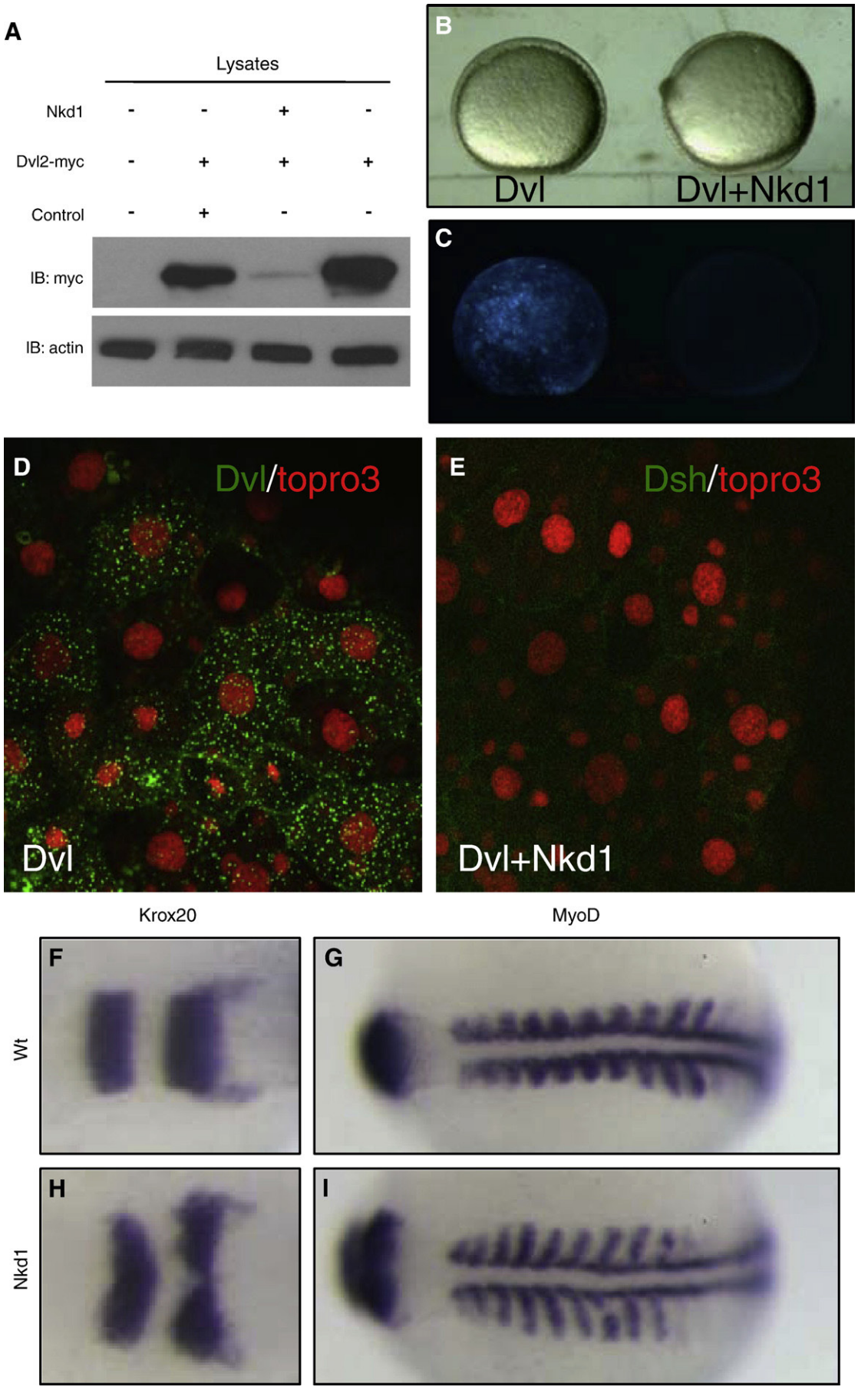
A
Lysates
Nkd1 - - + -
Dvl2-myc - + + +
Control - + - -
IB: myc
IB: actin
B
Dvl
Dvl+Nkd1
C
D
Dvl/topro3
Dvl
E
Dsh/topro3
Dvl+Nkd1
Krox20
MyoD
Wt
Nkd1
F
G
H
I

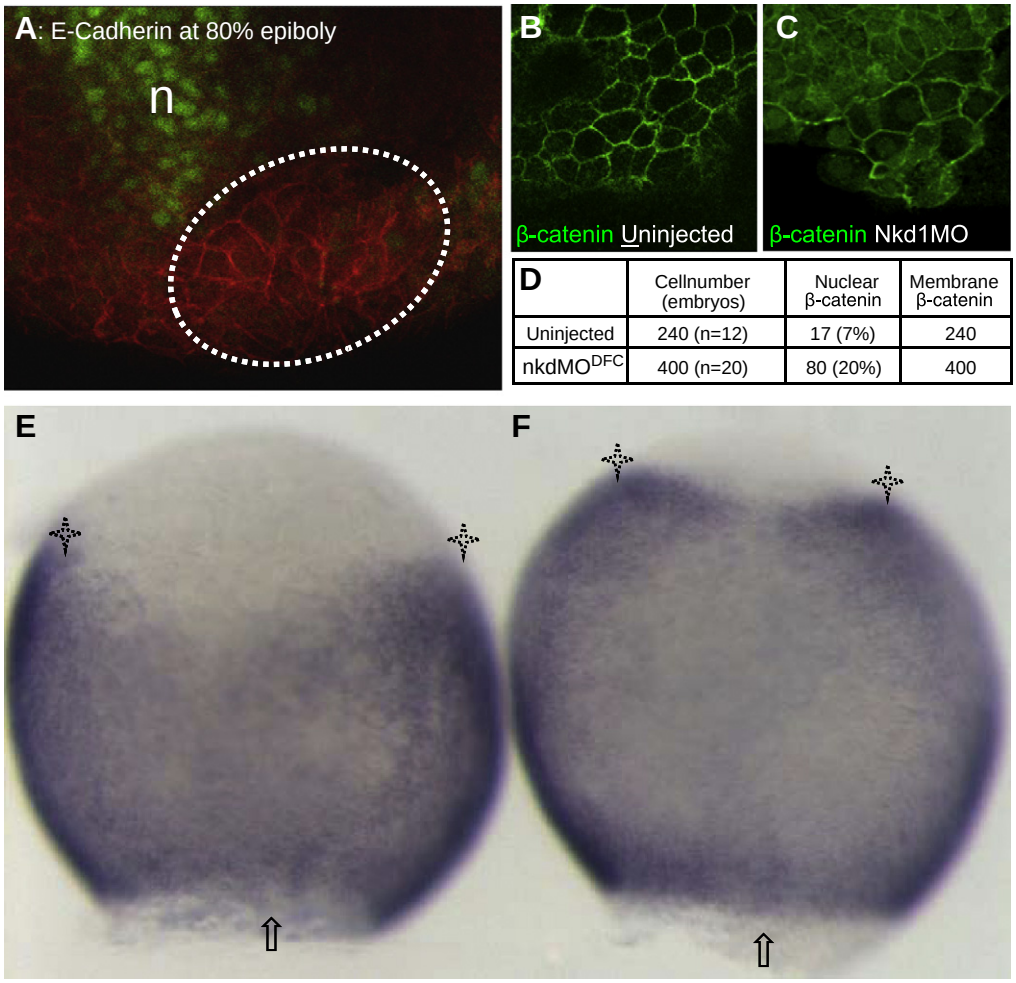

D	Cellnumber (embryos)	Nuclear β-catenin	Membrane β-catenin
Uninjected	240 (n=12)	17 (7%)	240
nkdMO^{DFC}	400 (n=20)	80 (20%)	400

Fig. 7. Nkd1 knockdown promotes nuclear β-catenin accumulation in DFCs and activates β-catenin transcriptional targets. Immunohistochemistry on embryos at 80% epiboly. (A) The DFC region (dashed lines) was identified by the position relative to the gsc-GFP positive region (green) and yolk, cell membrane is noted by E-cadherin distribution. (B) In wt DFC, β-catenin is detected mostly in plasma membrane. (C) In Nkd1MO^{DFC} embryos, β-catenin is detected at the plasma membrane and in the nuclei of cells in DFC cluster. (D) Summary of β-catenin-positive nuclei present in DFCs of wt and Nkd1MO^{DFC} embryos. n = notochord. *$P < 6.8 \times 10^{-6}$, Fisher's exact test. WMISH of axin2, dorsal side shown. (E) *axin2* expression is excluded from the DFC region (arrow) with distinct lateral domains (asterisks) in ControlMO^{DFC} embryos. (F) Expanded axin2 expression is detected in Nkd1MO^{DFC} embryos. 91% show expanded domains, n = 33 compared to 7% in control MO, n = 27 (p-value = 2.1×10^{-11}).

A prominent feature of Nkd protein is a single EF-hand. EF hands are conserved Ca^{2+}-binding motifs that usually occur in adjacent pairs, but have been observed in other configurations (Kawasaki et al., 1998). The EF-hand motif present in Nkd is most similar to the high-affinity Ca^{2+}-binding EF-hand 3 of the recoverin family of myristoyl switch proteins (Zeng et al., 2000). An unusual pair of histidine residues that may impair ion binding is present in the EF-hand motif of *Drosophila* Nkd, but not in vertebrate Nkds (Wharton et al., 2001). As expected, the Nkd EF-hand is required for Wnt/β-catenin antagonism in mammals (Yan et al., 2001), but dispensable in *Drosophila* (Rousset et al., 2002) and there is no identified role for Nkd in *Drosophila* PCP signaling. In contrast, zebrafish Nkd displays the distinctive property of affecting both β-catenin-dependent and -independent branches of the network (Van Raay et al., 2007). Therefore, the zebrafish Nkd1 could be functioning downstream of Ca^{2+}, as a sensor, to translate Ca^{2+} fluxes into β-catenin antagonism and LR patterning. Despite the conservation of key residues in the EF-hand motif, there is no evidence that Nkd proteins bind to Ca^{2+} or if binding is central to Nkd function (Hu et al., 2006). However, EF-hand deletion or point mutations in putative ion-binding residues of mouse Nkd1 still bind Dvl, but lose the ability to antagonize Wnt/β-catenin activity as evaluated by overexpression assays in *Xenopus* (Yan et al., 2001). Curiously, mouse knockout studies do not reveal any significant embryonic defects (Zhang et al., 2007). Whether Nkd1 acts downstream or in conjunction with Ca^{2+} release in DFC is yet to be determined.

A subset of KV cells express the Nodal antagonist *charon*. While *charon* function is crucial for proper LR patterning (Hashimoto et al., 2004), regulation of *charon* expression around the KV remains unclear. *charon* expression (but not KV formation) can be blocked by knockdown of Fgf8 (Hong and Dawid, 2009) or by inhibition of Notch signaling, consistent with the presence of Su (H)/CSL binding motifs upstream of the *charon* promoter (Gourronc et al., 2007). However, the functional relationships, if any, between the various pathways implicated in *charon* expression are not yet resolved. Our analysis revealed a right-sided *charon* expression bias in wt and control embryos, whereas Nkd1MO^{DFC} embryos have reduced KV cilia

Fig. 6. Nkd1 promotes Dvl degradation and impacts CE movements. (A) Westerm blot of zebrafish embryos injected with myc-tagged Dvl2 only, or coinjected with either *nkd1* RNA or *egfp* RNA. The first lane is uninjected embryos, anti-β-actin was used as loading control. Embryos were frozen at 80% epiboly and equal amounts of cell lysates were used for Western blot analysis. (B) Bright field and (C) fluorescence images of embryos at 90% epiboly, injected with Dvl-GFP only (left) or coinjected with *nkd1* RNA (right). (D) Dvl-GFP (green) and Topro3 nuclear staining (red) denotes Dvl localization in wt and (E) Dvl-GFP coinjected with *nkd1* RNA. (F) *krox20* and (G) *myoD* markers in uninjected and (H) *krox20* and (I) *myoD* markers *nkd1* RNA-injected zebrafish embryos. 43% of *nkd1* injected embryos show CE defects, n = 143. Dorsal view, anterior to the left.

and unbiased *charon* expression around the KV leading to aberrant expression of LR molecular markers and disrupted organ laterality. Exogenous Nkd1 was able to significantly restore asymmetric *charon* distribution when coinjected with Nkd1MO^{DFC} in embryos.

The Nkd1MO^{DFC} induced *charon* defect could be the result of reduced KV size, loss of KV cilia or both. By independently targeting three ciliary proteins, Invs, Sea and Ift88, we show that *charon* asymmetry around the KV is cilia-dependent. These results suggest a mechanism for loss of *charon* asymmetry in Nkd1MO^{DFC} embryos, which could be, at least in part, a result of loss of KV cilia.

In conclusion, we provide evidence that zebrafish Nkd1 can destabilize Dvl and is required for antagonism of Wnt signaling in DFCs, proper DFC migration, KV formation, cilia-mediated *charon* asymmetry and ultimately LR patterning.

Supplementary data to this article can be found online at doi:10.1016/j.ydbio.2010.08.040.

Acknowledgments

We thank members of the Slusarski lab and the Houston lab for helpful discussions and Dr. Michael Rebagliati for comments on the manuscript. This work was supported by grants from the NIH (CA112369 to DCS) and an American Heart Association Pre-doctoral fellowship to I.S.

Competing interests statement: The authors declare no competing financial interests.

References

Ahmad, N., Long, S., Rebagliati, M., 2004. A southpaw joins the roster: the role of the zebrafish nodal-related gene southpaw in cardiac LR asymmetry. Trends Cardiovasc. Med. 14, 43–49.

Amack, J.D., Yost, H.J., 2004. The T box transcription factor no tail in ciliated cells controls zebrafish left–right asymmetry. Curr. Biol. 14, 685–690.

Amores, A., Force, A., Yan, Y.L., Joly, L., Amemiya, C., Fritz, A., Ho, R.K., Langeland, J., Prince, V., Wang, Y.L., Westerfield, M., Ekker, M., Postlethwait, J.H., 1998. Zebrafish hox clusters and vertebrate genome evolution. Science 282, 1711–1714.

Antic, D., Stubbs, J.L., Suyama, K., Kintner, C., Scott, M.P., Axelrod, J.D., 2010. Planar cell polarity enables posterior localization of nodal cilia and left–right axis determination during mouse and Xenopus embryogenesis. PLoS ONE 5, e8999.

Bisgrove, B.W., Snarr, B.S., Emrazian, A., Yost, H.J., 2005. Polaris and Polycystin-2 in dorsal forerunner cells and Kupffer's vesicle are required for specification of the zebrafish left–right axis. Dev. Biol. 287, 274–288.

Cooper, M.S., D'Amico, L.A., 1996. A cluster of noninvoluting endocytic cells at the margin of the zebrafish blastoderm marks the site of embryonic shield formation. Dev. Biol. 180, 184–198.

Creyghton, M.P., Roel, G., Eichhorn, P.J., Hijmans, E.M., Maurer, I., Destree, O., Bernards, R., 2005. PR72, a novel regulator of Wnt signaling required for Naked cuticle function. Genes Dev. 19, 376–386.

Doitsidou, M., Reichman-Fried, M., Stebler, J., Koprunner, M., Dorries, J., Meyer, D., Esguerra, C.V., Leung, T., Raz, E., 2002. Guidance of primordial germ cell migration by the chemokine SDF-1. Cell 111, 647–659.

Dorsky, R.I., Sheldahl, L.C., Moon, R.T., 2002. A transgenic Lef1/beta-catenin-dependent reporter is expressed in spatially restricted domains throughout zebrafish development. Dev. Biol. 241, 229–237.

Essner, J.J., Amack, J.D., Nyholm, M.K., Harris, E.B., Yost, H.J., 2005. Kupffer's vesicle is a ciliated organ of asymmetry in the zebrafish embryo that initiates left–right development of the brain, heart and gut. Development 132, 1247–1260.

Freisinger, C.M., Schneider, I., Westfall, T.A., Slusarski, D.C., 2008. Calcium dynamics integrated into signalling pathways that influence vertebrate axial patterning. Philos. Trans. R. Soc. Lond. B Biol. Sci. 363, 1377–1385.

Gourronc, F., Ahmad, N., Nedza, N., Eggleston, T., Rebagliati, M., 2007. Nodal activity around Kupffer's vesicle depends on the T-box transcription factors Notail and Spadetail and on Notch signaling. Dev. Dyn. 236, 2131–2146.

Guo, J., Cagatay, T., Zhou, G., Chan, C.C., Blythe, S., Suyama, K., Zheng, L., Pan, K., Qian, C., Hamelin, R., Thibodeau, S.N., Klein, P.S., Wharton, K.A., Liu, W., 2009. Mutations in the human naked cuticle homolog NKD1 found in colorectal cancer alter Wnt/Dvl/beta-catenin signaling. PLoS ONE 4, e7982.

Hamada, H., Meno, C., Watanabe, D., Saijoh, Y., 2002. Establishment of vertebrate left-right asymmetry. Nat. Rev. Genet. 3, 103–113.

Hashimoto, H., Rebagliati, M., Ahmad, N., Muraoka, O., Kurokawa, T., Hibi, M., Suzuki, T., 2004. The Cerberus/Dan-family protein Charon is a negative regulator of Nodal signaling during left-right patterning in zebrafish. Development 131, 1741–1753.

Hojo, M., Takashima, S., Kobayashi, D., Sumeragi, A., Shimada, A., Tsukahara, T., Yokoi, H., Narita, T., Jindo, T., Kage, T., Kitagawa, T., Kimura, T., Sekimizu, K., Miyake, A., Setiamarga, D., Murakami, R., Tsuda, S., Ooki, S., Kakihara, K., Naruse, K., Takeda, H., 2007. Right-elevated expression of charon is regulated by fluid flow in medaka Kupffer's vesicle. Dev. Growth Differ. 49, 395–405.

Hong, S.K., Dawid, I.B., 2009. FGF-dependent left-right asymmetry patterning in zebrafish is mediated by Ier2 and Fibp1. Proc. Natl Acad. Sci. USA 106, 2230–2235.

Hu, T., Krezel, A.M., Li, C., Coffey, R.J., 2006. Structural studies of human Naked2: a biologically active intrinsically unstructured protein. Biochem. Biophys. Res. Commun. 350, 911–915.

Hu, T., Li, C., Cao, Z., Van Raay, T.J., Smith, J.G., Willert, K., Solnica-Krezel, L., Coffey, R.J., 2010. Myristoylated naked2 antagonizes WNT-{beta}-catenin activity by degrading dishevelled-1 at the plasma membrane. J. Biol. Chem.

Huang, H., He, X., 2008. Wnt/beta-catenin signaling: new (and old) players and new insights. Curr. Opin. Cell Biol. 20, 119–125.

Huang, P., Schier, A.F., 2009. Dampened Hedgehog signaling but normal Wnt signaling in zebrafish without cilia. Development 136, 3089–3098.

Jaillon, O., Aury, J.M., Brunet, F., Petit, J.L., Stange-Thomann, N., Mauceli, E., Bouneau, L., Fischer, C., Ozouf-Costaz, C., Bernot, A., Nicaud, S., Jaffe, D., Fisher, S., Lutfalla, G., Dossat, C., Segurens, B., Dasilva, C., Salanoubat, M., Levy, M., Boudet, N., Castellano, S., Anthouard, V., Jubin, C., Castelli, V., Katinka, M., Vacherie, B., Biemont, C., Skalli, Z., Cattolico, L., Poulain, J., De Berardinis, V., Cruaud, C., Duprat, S., Brottier, P., Coutanceau, J.P., Gouzy, J., Parra, G., Lardier, G., Chapple, C., McKernan, K.J., McEwan, P., Bosak, S., Kellis, M., Volff, J.N., Guigo, R., Zody, M.C., Mesirov, J., Lindblad-Toh, K., Birren, B., Nusbaum, C., Kahn, D., Robinson-Rechavi, M., Laudet, V., Schachter, V., Quetier, F., Saurin, W., Scarpelli, C., Wincker, P., Lander, E.S., Weissenbach, J., Roest Crollius, H., 2004. Genome duplication in the teleost fish Tetraodon nigroviridis reveals the early vertebrate proto-karyotype. Nature 431, 946–957.

Katoh, M., 2001. Molecular cloning, gene structure, and expression analyses of NKD1 and NKD2. Int. J. Oncol. 19, 963–969.

Kawasaki, H., Nakayama, S., Kretsinger, R.H., 1998. Classification and evolution of EF-hand proteins. Biometals 11, 277–295.

Keller, R., 2002. Shaping the vertebrate body plan by polarized embryonic cell movements. Science 298, 1950–1954.

Kimmel, C.B., W, B.W., Kimmel, S.R., Ullmann, B., F,S.T., 1995. Stages of embryonic development of the zebrafish. Dev. Dyn. 203, 253–310.

Kishimoto, N., Cao, Y., Park, A., Sun, Z., 2008. Cystic kidney gene seahorse regulates cilia-mediated processes and Wnt pathways. Dev. Cell 14, 954–961.

Kohn, A.D., Moon, R.T., 2005. Wnt and calcium signaling: beta-catenin-independent pathways. Cell Calcium 38, 439–446.

Kramer-Zucker, A.G., Olale, F., Haycraft, C.J., Yoder, B.K., Schier, A.F., Drummond, I.A., 2005. Cilia-driven fluid flow in the zebrafish pronephros, brain and Kupffer's vesicle is required for normal organogenesis. Development 132, 1907–1921.

Lin, X., Xu, X., 2009. Distinct functions of Wnt/beta-catenin signaling in KV development and cardiac asymmetry. Development 136, 207–217.

Marques, S., Borges, A.C., Silva, A.C., Freitas, S., Cordenonsi, M., Belo, J.A., 2004. The activity of the Nodal antagonist Cerl-2 in the mouse node is required for correct L/R body axis. Genes Dev. 18, 2342–2347.

Melby, A.E., Warga, R.M., Kimmel, C.B., 1996. Specification of cell fates at the dorsal margin of the zebrafish gastrula. Development 122, 2225–2237.

Molina, G.A., Watkins, S.C., Tsang, M., 2007. Generation of FGF reporter transgenic zebrafish and their utility in chemical screens. BMC Dev. Biol. 7, 62.

Nakaya, M.A., Biris, K., Tsukiyama, T., Jaime, S., Rawls, J.A., Yamaguchi, T.P., 2005. Wnt3a links left-right determination with segmentation and anteroposterior axis elongation. Development 132, 5425–5436.

Nonaka, S., Tanaka, Y., Okada, Y., Takeda, S., Harada, A., Kanai, Y., Kido, M., Hirokawa, N., 1998. Randomization of left-right asymmetry due to loss of nodal cilia generating leftward flow of extraembryonic fluid in mice lacking KIF3B motor protein. Cell 95, 829–837.

Ocbina, P.J.R., Tuson, M., Anderson, K.V., 2009. Primary Cilia Are Not Required for Normal Canonical Wnt Signaling in the Mouse Embryo. PLoS ONE 4, e6839.

Oishi, I., Kawakami, Y., Raya, A., Callol-Massot, C., Izpisua Belmonte, J.C., 2006. Regulation of primary cilia formation and left-right patterning in zebrafish by a noncanonical Wnt signaling mediator, duboraya. Nat. Genet. 38, 1316–1322.

Okada, Y., Takeda, S., Tanaka, Y., Belmonte, J.C., Hirokawa, N., 2005. Mechanism of nodal flow: a conserved symmetry breaking event in left-right axis determination. Cell 121, 633–644.

Oki, S., Kitajima, K., Marques, S., Belo, J.A., Yokoyama, T., Hamada, H., Meno, C., 2009. Reversal of left-right asymmetry induced by aberrant Nodal signaling in the node of mouse embryos. Development 136, 3917–3925.

Oteiza, P., Koppen, M., Concha, M.L., Heisenberg, C.P., 2008. Origin and shaping of the laterality organ in zebrafish. Development 135, 2807–2813.

Otto, E.A., Schermer, B., Obara, T., O'Toole, J.F., Hiller, K.S., Mueller, A.M., Ruf, R.G., Hoefele, J., Beekmann, F., Landau, D., Foreman, J.W., Goodship, J.A., Strachan, T., Kispert, A., Wolf, M.T., Gagnadoux, M.F., Nivet, H., Antignac, C., Walz, G., Drummond, I.A., Benzing, T., Hildebrandt, F., 2003. Mutations in INVS encoding inversin cause nephronophthisis type 2, linking renal cystic disease to the function of primary cilia and left-right axis determination. Nat. Genet. 34, 413–420.

Roszko, I., Sawada, A., Solnica-Krezel, L., 2009. Regulation of convergence and extension movements during vertebrate gastrulation by the Wnt/PCP pathway. Semin. Cell Dev. Biol. 20, 986–997.

Rousset, R., Mack, J.A., Wharton Jr., K.A., Axelrod, J.D., Cadigan, K.M., Fish, M.P., Nusse, R., Scott, M.P., 2001. Naked cuticle targets dishevelled to antagonize Wnt signal transduction. Genes Dev. 15, 658–671.

Rousset, R., Wharton Jr., K.A., Zimmermann, G., Scott, M.P., 2002. Zinc-dependent interaction between dishevelled and the Drosophila Wnt antagonist naked cuticle. J. Biol. Chem. 277, 49019–49026.

Schneider, I., Houston, D.W., Rebagliati, M.R., Slusarski, D.C., 2008. Calcium fluxes in dorsal forerunner cells antagonize beta-catenin and alter left-right patterning. Development 135, 75–84.

Schweickert, A., Weber, T., Beyer, T., Vick, P., Bogusch, S., Feistel, K., Blum, M., 2007. Cilia-driven leftward flow determines laterality in Xenopus. Curr. Biol. 17, 60–66.
Serluca, F.C., Xu, B., Okabe, N., Baker, K., Lin, S.Y., Sullivan-Brown, J., Konieczkowski, D.J., Jaffe, K.M., Bradner, J.M., Fishman, M.C., Burdine, R.D., 2009. Mutations in zebrafish leucine-rich repeat-containing six-like affect cilia motility and result in pronephric cysts, but have variable effects on left-right patterning. Development 136, 1621–1631.
Shimizu, T., Yamanaka, Y., Ryu, S.-L., Hashimoto, H., Yabe, T., Hirata, T., Bae, Y.-k., Hibi, M., Hirano, T., 2000. Cooperative roles of Bozozok/Dharma and Nodal-related proteins in the formation of the dorsal organizer in zebrafish. Mech. Dev. 91, 293–303.
Slusarski, D.C., Pelegri, F., 2007. Calcium signaling in vertebrate embryonic patterning and morphogenesis. Dev. Biol. 307, 1–13.
Solnica-Krezel, L., 2005. Conserved patterns of cell movements during vertebrate gastrulation. Curr. Biol. 15, R213–R228.
Sun, Z., Amsterdam, A., Pazour, G.J., Cole, D.G., Miller, M.S., Hopkins, N., 2004. A genetic screen in zebrafish identifies cilia genes as a principal cause of cystic kidney. Development 131, 4085–4093.
Taylor, J.S., Braasch, I., Frickey, T., Meyer, A., Van de Peer, Y., 2003. Genome duplication, a trait shared by 22000 species of ray-finned fish. Genome Res. 13, 382–390.
Topol, L., Jiang, X., Choi, H., Garrett-Beal, L., Carolan, P.J., Yang, Y., 2003. Wnt-5a inhibits the canonical Wnt pathway by promoting GSK-3-independent {beta}-catenin degradation. J. Cell Biol. 162, 899–908.
Van Raay, T.J., Coffey, R.J., Solnica-Krezel, L., 2007. Zebrafish Naked1 and Naked2 antagonize both canonical and non-canonical Wnt signaling. Dev. Biol. 309, 151–168.
Weidinger, G., Thorpe, C.J., Wuennenberg-Stapleton, K., Ngai, J., Moon, R.T., 2005. The Sp1-related transcription factors sp5 and sp5-like act downstream of Wnt/[beta]-catenin signaling in mesoderm and neuroectoderm patterning. Curr. Biol. 15, 489–500.
Westfall, T.A., Brimeyer, R., Twedt, J., Gladon, J., Olberding, A., Furutani-Seiki, M., Slusarski, D.C., 2003a. Wnt-5/pipetail functions in vertebrate axis formation as a negative regulator of Wnt/beta-catenin activity. J. Cell Biol. 162, 889–898.
Westfall, T.A., Hjertos, B., Slusarski, D.C., 2003b. Requirement for intracellular calcium modulation in zebrafish dorsal–ventral patterning. Dev. Biol. 259, 380–391.
Wharton Jr., K.A., Zimmermann, G., Rousset, R., Scott, M.P., 2001. Vertebrate proteins related to Drosophila Naked Cuticle bind Dishevelled and antagonize Wnt signaling. Dev. Biol. 234, 93–106.
Wright, C.V., Halpern, M.E., 2002. Specification of left–right asymmetry. Results Probl. Cell Differ. 40, 96–116.
Yan, D., Wallingford, J.B., Sun, T.Q., Nelson, A.M., Sakanaka, C., Reinhard, C., Harland, R.M., Fantl, W.J., Williams, L.T., 2001. Cell autonomous regulation of multiple Dishevelled-dependent pathways by mammalian Nkd. Proc. Natl Acad. Sci. USA 98, 3802–3807.
Zeng, W., Wharton Jr., K.A., Mack, J.A., Wang, K., Gadbaw, M., Suyama, K., Klein, P.S., Scott, M.P., 2000. naked cuticle encodes an inducible antagonist of Wnt signalling. Nature 403, 789–795.
Zhang, Y., Levin, M., 2009. Left–right asymmetry in the chick embryo requires core planar cell polarity protein Vangl2. Genesis 47, 719–728.
Zhang, S., Cagatay, T., Amanai, M., Zhang, M., Kline, J., Castrillon, D.H., Ashfaq, R., Oz, O.K., Wharton Jr., K.A., 2007. Viable mice with compound mutations in the Wnt/Dvl pathway antagonists nkd1 and nkd2. Mol. Cell. Biol. 27, 4454–4464.